Phenomenology of Photoinduced Processes in the Ionic Sol−Gel-Based Azobenzene Materials

Lazar Kulikovsky,[†] Olga Kulikovska,[†] Leonid M. Goldenberg,[†] and Joachim Stumpe*,[†],[‡]

Fraunhofer Institute for Applied Polymer Research, Science Campus Golm, Geiselbergstrasse 69, 14476 Potsdam, Germany, and Institute of Thin Film Technology and Microsensorics, Kanstrasse 55, 14513 Teltow, Germany

ABSTRACT Very recently, supramolecular azobenzene-containing materials have been demonstrated to be effective for holographic inscription of surface relief gratings. High efficiency of grating formation in these materials is advantageously combined with easy material preparation because of the supramolecular principle of building blocs combination, availability of chemical components, and good film-forming properties. The materials show great promise for wide optical applications. Here, one type of material formulation based on ionic complexes of poly(aminosiloxane) is experimentally investigated concerning the induction of birefringence, efficiency of relief formation, and thermal stability of surface structures. Properties of the material were changed on the molecular level by varying the azobenzene content and on the macro level by varying chemical processing conditions. The results are discussed in terms of cross-linking and plasticizing effects caused by residual solvent and the low-molecular-weight azobenzene component. An improvement of both the efficiency of grating formation and their thermal stability by these means has been demonstrated. The results can be adapted to other azobenzene-containing materials. In addition, a drastic change of films solubility has been observed upon irradiation.

KEYWORDS: azobenzene • ionic interactions • polysiloxane • surface relief gratings • holography • diffraction

1. INTRODUCTION

The potential use of azo (aromatic) photochromes in photonic applications has motivated investigations of their optical properties and, on the other hand, brought about a variety of azobenzene-containing materials. Such attention is due to their photochromic and nonlinear properties, photoinduced anisotropy, and not least to the light-induced formation of surface relief gratings (SRG) (1). Optical anisotropy arises from the angular orientation of the chromophores in the film bulk, whereas the formation of SRG implies an undulation of the film surface due to light-induced translation motions of the azobenzene moieties. Both rotation and translation of azobenzene units can induce motion of further molecular segments or of the whole macromolecules. A basic effect enabling the motion of the azobenzene moieties in solid films is their $E-Z$ photoisomerization. Upon irradiation with polarized light it results in the preferential orientation of chromophores perpendicularly to the electric field vector of the irradiating light. The orientation process has been well-investigated in a variety of materials and applications. The nature of the light-induced mass transport upon spatially inhomogeneous irradiation is not clear so far and possible explanations go from the statistical diffusion of chromophores to pressure or stress gradients. All models consider the $E-Z$ photoisomerization as necessary condition. The extent of interdependence of the molecular orientation and translation motion is still disputed. The up-to-date discussion on the azobenzene-containing materials and photoinduced processes can be found in a recent book (2).

Both stable and dynamic anisotropy including birefringence gratings have been widely investigated in a variety of materials (3–6). The formation of SRG has been mostly investigated in films of azobenzene functionalized polymers as presented in early reviews (3, 7), including hybrid sol−gel matrices (8, 9). It has been also demonstrated in doped systems (10), LB and layer-by-layer (LbL) films (5), and low-molecular-weight film-forming materials (11).

The covalent bonding of azobenzene to the polymer chains has been considered as a means of high azobenzene loading, a stabilizing factor for the induced molecular orientation (8), and as an essential condition for effective mass transport (7, 12). Rather unexpectedly, an extremely effective formation of SRG in supramolecular polymer materials, where the chromophores are attached to the passive polyelectrolyte backbones by noncovalent interactions, has been demonstrated. Relief gratings (1650 nm deep) were readily formed using ionic complexes of oppositely charged azobenzene derivatives and polyelectrolytes (13, 14), including polyelectrolytes formed by in situ sol−gel reaction (15). Moreover, the effective formation of SRG in these materials is combined with their high thermal and long-term stability. Also, the materials with hydrogen-bondings were capable
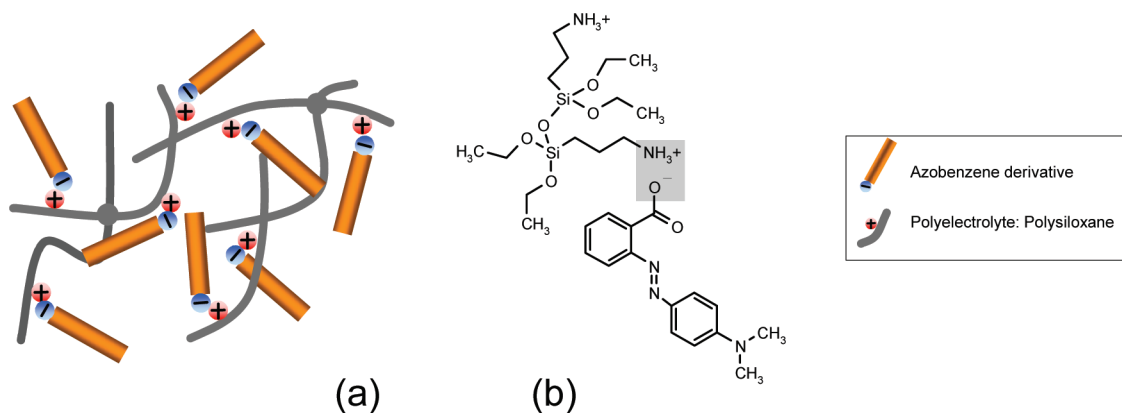

FIGURE 1. (a) Schematic presentation of an azobenzene-based supramolecular sol−gel material with ionic interactions; (b) an example of complex formation between APTES dimer and one molecule of methyl red corresponding to the material with MR:APTES molar ratio 0.5:1.

of stable photoinduced orientation and of SRG formation (16, 17). Because of its simplicity and versatility, the supramolecular approach has reopened application prospects for the light-induced mass transport in azobenzene-containing materials.

The supramolecular materials based on sol−gel reaction differ from other supramolecular systems reported in the literature for the SRG formation. In these materials, the irreversible cross-linking of polymer backbones due to the formation of a polysiloxane network by polycondensation is possible. In contrary to the sol−gel materials with grafted azobenzenes (9, 18, 19), where the cross-linking has been reported to hinder the SRG formation (9, 18), in the case of ionic sol−gel materials, some degree of cross-linking was considered rather as a stabilizing factor (15). It was suggested that if the material is not rigid enough, the induction of any ordered structures will be counteracted by some relaxation processes, resulting in a less effective formation of SRG and their poor stability. At the same time, the cross-linking invests the SRG with some irreversibility. Either way, the cross-linking process and the ionic bonding of chromophores have a share in photoinduced processes in this material.

In the present work, we study the photoinduced processes in the supramolecular material based on sol−gel reaction schematically presented in Figure 1. The detailed investigation on the photoinduced birefringence and SRG in this material is presented. We tried to approach the topic multilaterally and therefore involved in the consideration some parameters like solvent (water) content, plasticization effects, etc. that have been rather undervalued in the literature on SRG. The ratio of MR:APTES was varied in a wide range, namely up to 4:1. For the first time, the photoinduction and thermal stability of SRG were investigated in dependence on the MR:APTES ratio in such a wide range. Another issue addressed in this study is a photoinduction of birefringence. We report here how the value of the induced birefringence and particularly the residual birefringence in this material may be influenced by film pretreatment. The influence of the film pretreatment on the thermal stability of SRG is also reported. Furthermore, we report on the first observation of an additional effect observed in these materials upon irradiation with light where the irradiated films become insoluble. The discussion of these phenomena under consideration of macroscopic film properties is strongly related to possible tuning of the material properties and creating tailored materials for different applications.

2. EXPERIMENTAL SECTION

Materials. Chemical formulas of the components are displayed in Figure 1 b, where a complex of siloxane dimer with one molecule of dye is shown as an example.

Ninety milligrams (0.3 mmol) of 2-(4-dimethylaminophenylazo)benzoic acid, Na salt (further MR) in 2 mL of MeOH was mixed with 70 μL (0.3 mmol) of 3-aminopropyltriethoxysilane (APTES, Witco Europa SA). After addition of 20 μL (0.3 mmol, stoichiometric ratio to APTES) of concentrated HCl, the solution was filtrated through a 0.2 μm Nalgene filter and used for the film preparation. The formulation with smaller (catalytic) concentration of HCl was prepared similarly according to ref 20. The molar ratio MR:APTES has been varied between 0.5:1 and 4:1, thus achieving dye loading of 84 % by weight. This was possibly due to the very good solubility of MR in MeOH. The complex presented schematically in Figure 1b is an example with a complexation degree of 0.5 (MR:APTES molar ratio 0.5:1).

The films of 1−2 μm thickness were prepared from the above-described solutions by spin-coating onto glass substrates at 1000−3000 rpm. For FTIR spectral characterization, the films were spin-coated onto Si substrates. Typically the spin-coated films were then heated in oven at 70 °C for 30 min. Optically clear films were obtained for all formulations.

For the investigation of photoinduced birefringence, different drying procedures were additionally applied to the films. Namely, drying in a vacuum at room temperature using a vacuum desiccator with pressure of about 1×10^4 Pa, drying in deep vacuum of about 1 Pa with cooling at $t = -40$ °C using the lyophilic dryer Gamma 2−20 (Christ, Germany) and drying in oven at 70 °C and alternatively at 170 °C.

Measurements. FTIR measurements were performed in reflection mode at oblique incidence (angle of 60°) using Nexus 470 spectrometer (Thermo Nicolet, USA).

For induction of optical anisotropy the films were irradiated homogeneously with extended beam of an Ar$^+$ ion laser at the wavelength of 488 nm. The beam was polarized linearly with polarization plane at 45° and its intensity was equal to 1400 mW/cm^2. The induced optical anisotropy was probed by the weak beam of a He−Ne laser at 633 nm polarized linearly horizontally. By means of Wollaston prism the transmitted
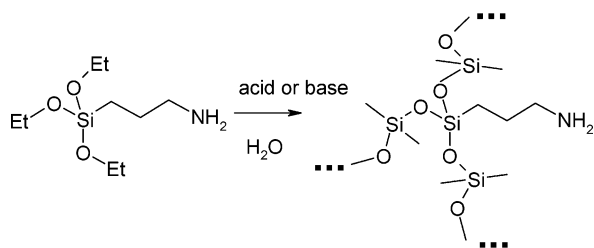
FIGURE 2. Schematic presentation of a possible cross-linked structure by the sol−gel reaction in APTES.

FIGURE 3. Experimental setup used for induction and measurement of birefringence: P, polarizer; HWP, half wave plate; ADC/DAC, analog-digital/digital-analog converter.

beam was divided into two beams polarized parallel and orthogonal to the polarization plane of the incident beam. The intensities of both parallel and orthogonal polarization components were measured.

For SRG inscription, the films were irradiated with the interference pattern of two orthogonally polarized beams from an Ar$^+$ ion laser operating at the wavelength of 488 nm. The beams were polarized linearly with polarization planes at ±45° to the incidence plane unless otherwise noted. An angle between two interfering beams was typically about 16°, resulting in a period of 1.7 μm. The intensities of irradiating beams were ca. 400 mW/cm^2.

The grating formation was probed by diffraction of a weak probe beam from a He−Ne laser. The intensities of zeroth, ±first and ±second diffraction orders were measured during grating recording.

The SRG were verified by atomic force microscopy performed at Solver P47H Smena (NTMDT) in semicontact mode.

The thermal stability of SRG was investigated using a heating stage RCT-B (IKA). The samples with inscribed gratings were annealed for 10 min at each temperature. The temperature of the film was measured by means of a thermocouple. The diffraction intensities of gratings were measured after each annealing step.

3. RESULTS AND DISCUSSION

Materials investigated here are ionic complexes of azobenzene derivatives and polyelectrolytes (Figure 1), whereas the latter is formed by in situ sol−gel reaction. We have reported earlier that no T$_g$ was observed for these materials (15). We have been using 3-aminopropyltriethoxysilane (APTES), an alkoxysilane molecule with three alkoxy-subsituents. As all alkoxysilanes APTES is capable of polycondensation. If possessing at least three alkoxy-subsituents, it is capable not only of building linear products but also cross-linked ones, which is schematically depicted in Figure 2. The condensation reaction is manifested in IR spectra of the film, where instead of a single peak at 1090 cm^{-1} in a starting siloxane component (APTES) assigned to Si−O−C stretching vibrations, two additional peaks at 1065 and 1125 cm^{-1} appear in the spectra of investigated films that can be assigned according to the literature (21) to Si−O−Si stretching vibrations in the condensation product. Similarly, a weak vibration of silanol Si−O(H) groups of intermediate moieties was observed at 920 cm^{-1} (9). In this work, the degree of condensation was easily controlled by the drying−heating process. The achieved degree of condensation or, if applicable, of partial cross-linking should increase the rigidity of the matrix.

3.1. Photoinduction and Relaxation of Birefringence Dependent on the Film Pretreatment. The optical anisotropy is induced in azobenzene containing
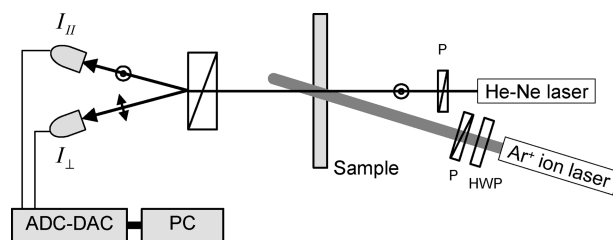
materials simultaneously, if not previously, to the SRG formation. Thus photo-orientation has been considered by some authors to be intrinsically connected to the translation molecular movement (12). For both processes, the type of connection of chromophore to the polymer matrix seems to be essential. For example, it was reported that covalent bonding stabilizes the photoinduced molecular order and favors the mass transport (5, 8, 12, 22). The effect of the ionic bonding on the stability of induced order is not ambiguous. In LbL systems formed by ionic interactions, it has been shown to prevent relaxation of photoinduced chromophores orientation (5). Extremely high and stable orientation was also induced in liquid crystalline azobenzene-containing ionic self-assembled complexes (6). At the same time birefringence induced in films of the azobenzene−polyelectrolyte ionic complexes was unstable (13).

Whereas the inscription of SRG in the materials under study was very effective, no significant birefringence could be induced at the similar experimental conditions. Notice for comparison that dynamic birefringence was easily induced in the azobenzene-polyelectrolyte complexes (13). Also in a liquid crystalline azobenzene-polyelectrolyte ionic complex a very high and stable photoinduced birefringence has been reported (17). Thus the ionic interactions alone can not be responsible for this observation. Here, we changed the residual solvent content and the degree of condensation by different pretreatment of films and investigated their effect on the photoinduction of birefringence. All films for this experiment were spin-coated from the same solution at the same conditions and had very similar thicknesses. Four different pretreatment procedures were then applied to the films: (1) drying at the room temperature and pressure of about 1 × 10^4 Pa for 20 h; (2) freezing in a lyophilic dryer at a $t = -40$ °C and a deep vacuum of about 1 Pa for 14 h; (3) heating at 70 °C for 30 min; and (4) heating at 70 °C for 30 min and then at 170 °C for 5 min. The samples were then irradiated with linearly polarized light at 488 nm and the induced birefringence was measured using setup shown in Figure 3. The expanded and spatially filtered irradiating laser beam passed through the polarizer at 45° to the incidence plane. A weak probe beam from a He−Ne laser at a wavelength of 633 nm was polarized linearly in the incidence plane, i.e., horizontally. After passing the sample it was divided by means of a Wollaston prism into two beams polarized horizontally and vertically. The intensities of both polarization components−with polarizations parallel $I_{\parallel}$ and orthogonal $I_{\perp}$ to the incident one−were measured
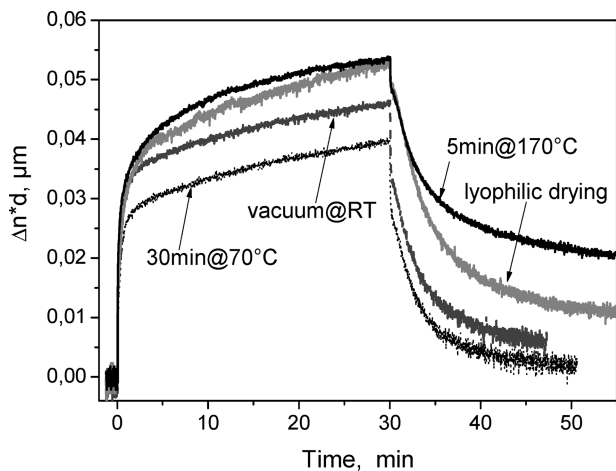
FIGURE 4. Photoinduction and relaxation of birefringence in a film with a ratio MR:APTES of 1.5:1.

during and after irradiation. The induced birefringence Δn may be calculated using the following formula

$$\frac{I_\perp}{I_\perp + I_{II}} = \sin^2 \frac{\pi \Delta n d}{\lambda \cos \Theta} \tag{1}$$

where d is film thickness, λ is probe wavelength, and Θ is incidence angle.

Figure 4 presents kinetics of the induction and relaxation of birefringence. As far as the thicknesses of all films were equal, the data in Figure 4 represent the induced birefringence. As is seen, birefringence was induced in all films after additional drying or heating, although its values remained rather small. The birefringence relaxed after switching off the irradiating light. A few differences in the induction and relaxation behavior are clearly seen. Slightly higher values of birefringence were reached in the film heated at higher temperature and in the frozen film dried in a deep vacuum. Moreover, the induced birefringence relaxes much slower in these films, remaining at the residual level of 40 and 20 % of the initially induced values for the heated and frozen films respectively. Thus both thermal and vacuum treatments have changed the birefringence induction and relaxation behavior, indicating that the photoinduced molecular orientation depends not only on the bonding type but also on the local surroundings of the azobenzene units. Probably, slow relaxation correlates with better molecular orientation and may be related to the spacial confinement of the azobenzene moieties. Faster relaxation indicates higher rotational freedom. Further in this study, we try to clarify to what extent this consideration may be applied to the formation of SRG and its thermal stability.

3.2. Holographic Inscription of SRG.
For inscription of SRG, the films were spin-coated onto glass slides and heated at 70 °C for 30 min. SRG were recorded by irradiating films with interference pattern of two laser beams at a wavelength of 488 nm, orthogonal polarizations and the intensities of 400 mW/cm². The holographic setup is shown in Figure 5. Formation of the grating was monitored by a weak linearly horizontally polarized probe beam at 633 nm,
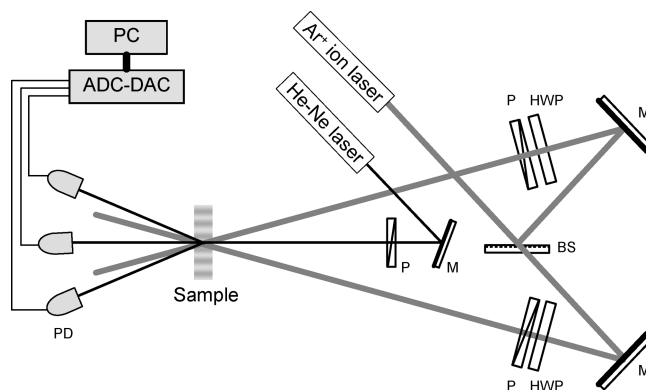

FIGURE 5. Holographic setup for induction of SRG: BS, beam splitter; M, mirror; P, polarizer; HWP, half wave plate; PD, photodiode; ADC/DAC, analog-digital/digital-analog converter.

where the absorption of films is low and the low power probe light does not influence the gratings. The diffraction efficiency of nth diffracted order was calculated as $\eta_n = I_n / \Sigma I_n$, where I_n are the intensities of the nth-order diffracted beams. Total diffraction efficiency was determined as the sum of diffraction efficiencies of all nonzero orders $\eta_{tot} = \eta_{\pm 1} + \eta_{\pm 2} + ...$; characterizing the recorded gratings by their total diffraction efficiencies proved an advantage especially in the case of deep surface gratings having many diffraction orders in the Raman−Nath regime of diffraction. A typical example of the recording kinetics is shown in Figure 6a. Under the above experimental conditions, five diffracted orders were observed. The first-order diffraction efficiency of 38 % was reached after 4 min of recording and reveals a notably high inscription rate. Ninety-eight percent of the probe light (η_{tot}) was diffracted by the recorded grating after less than 6 min. Such high diffraction efficiency can be explained only by the high modulation depth of the recorded relief grating. Indeed, a grating height of about 750 nm was confirmed by AFM measurements. The surface topology and the cross-section of the grating are shown in panels b and c in Figure 6. The period of the grating was measured to be 2 μm, in accordance with the period of the interference pattern. The achieved modulation depth is quite high in comparison to most azobenzene-containing materials; typically, the modulation depths in the range of a few hundreds nanometers have been reported (23). However, the superior modulation depth, as high as 1650 nm, was achieved by us in other types of supramolecular material (13).

3.3. Thermal and Time Stability of SRG.
Recorded gratings remain stable if kept at room conditions. It was verified by measurements of diffraction efficiencies after 2 months. Furthermore, we investigated thermal stability of the gratings. Generally speaking, SRG in covalently bound azobenzene-containing polymer are thermally stable below the glass transition temperature, which lies typically in the range of 40−150 °C (3). Reported polymers with high glass transition temperature (up to 150 °C) exhibited rather low SRG efficiency. We reported on the efficient and extremely thermally stable (up to 200 °C) SRG in a polymer material with ionic groups (24). Here, thermal stability study was done under the following assumptions: (i) aging of films
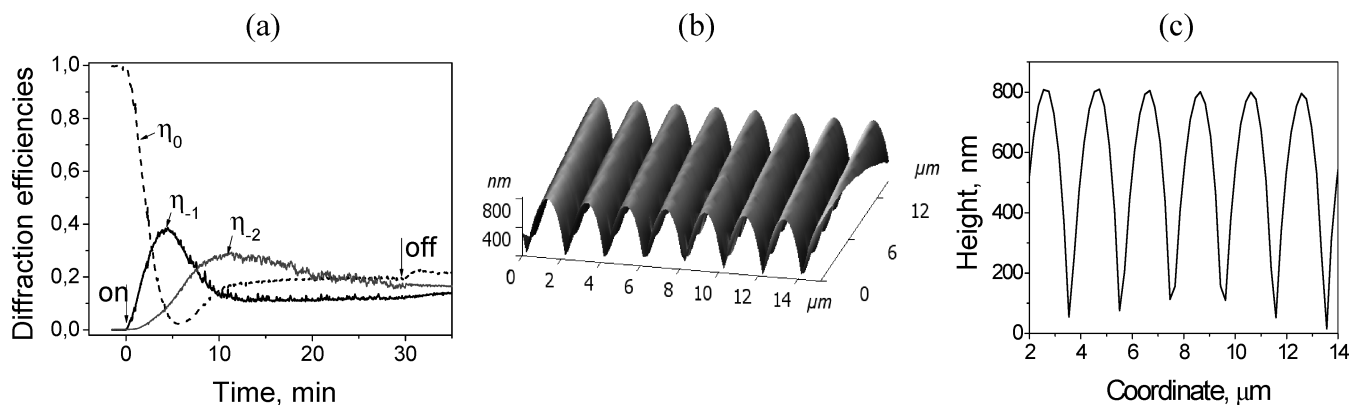
FIGURE 6. (a) Diffraction efficiencies; measured by (b) AFM surface topology and (c) corresponding cross-section of a grating inscribed in a film with MR:APTES ratio of 1.5:1 with catalytic amount of HCl.
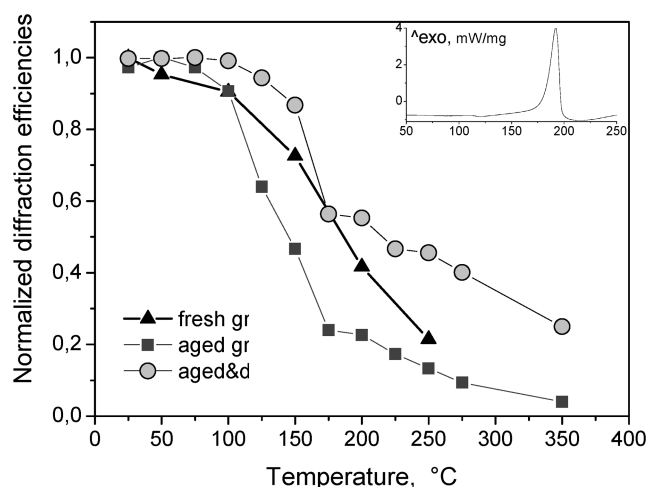

FIGURE 7. Thermal erasing of gratings in films with MR:APTES ratio of 1.5:1, normalized total diffraction efficiencies in dependence on the annealing temperatures: fresh grating (triangles); aged grating (filled squares); and aged grating that was then annealed at 70 °C for 4 h (filled circles). Inset: DSC curve (first heating) for material with MR:APTES ratio of 1.5:1.

results in a further condensation; (ii) the development of sol–gel condensation affects the stability of the induced relief structures; (iii) residual solvent content or water acts as plasticizer and thus can also influence the thermal stability. Correspondingly, the erasure behavior of SRG has been investigated for differently aged gratings, namely the gratings just after recording, the gratings aged at room conditions for 1 month, and the gratings aged for 1 month and then heated at 70 °C for 4 h. The latter temperature was chosen in correlation with the DSC curve, where a weak endothermic peak observed at the temperature of about 110 °C during the first heating was presumably related to the polycondensation reaction (Figure 7) (15). Most likely, the heating at 70 °C, well below the peak temperature, can result in further formation of the network but can not erase the induced grating. It was verified that the diffraction efficiency of the grating after heating at 70 °C for 4 h remained unchanged.

In this study, the erasure of gratings was phased by heating the samples on the heating stage at each temperature T for 10 min, starting from $T = 25$ °C and up to $T = 350$ °C with a step of $\Delta T = 25°$. Each heating step led to

the partial erasure of gratings. The degree of the partial erasure was estimated from diffraction of the probe beam at 633 nm measured after each heating step. The total diffraction efficiencies of annealed gratings normalized to the diffraction efficiencies of the gratings after recording $\eta_{norm} = \eta_{t°}/\eta_{rec} \times 100\%$ in dependence on the annealing temperatures are presented in Figure 7. In the temperature range below 110 °C, all gratings remained similarly stable. The erasing began at higher temperatures. It can be seen that this decrease in diffraction efficiency is essentially different if the gratings were erased directly after recording and if they were aged before the erasure. Both aged gratings show characteristic features at temperatures of about 190 °C. This feature (break) is absent in the erasure process of fresh gratings. The difference may be related to the degree of condensation that obviously is more developed in the aged films. Interestingly, the characteristic temperature of 190 °C correlates with the DSC curve, where a strong exothermic peak was measured at this temperature (Figure 7) (15). Beside a similarity of the erasure processes, both aged gratings reveal a significant difference concerning the remaining values of diffraction efficiencies. Heating the samples to 200 °C erased the aged grating to 23% of its initial value. At the same time, the diffraction efficiency of the aged and dried grating remained at a level of 55%. It is worth noticing here that this grating could not be completely erased, even by heating up to 350 °C, retaining 25% of its initial value.

The results show that the thermal stability of SRG in the ionic sol–gel materials is a function of time–thermal history of the sample, which may be assigned to the extended formation of the sol–gel network. This in turn is important for applications, where the adapted thermal post treatment can be used to stabilize the photoinduced gratings.

3.4. Variation of Dye MR:APTES Ratio.
We have also investigated the formation of SRG and its thermal stability in dependence on the MR:APTES ratio. It should be noticed here that the high loading level of azobenzene chromophores without aggregation and segregation is a general problem. The prevention of dye aggregation is one of the key challenges of functionalized polymers. For example, in the guest–host systems the aggregation has
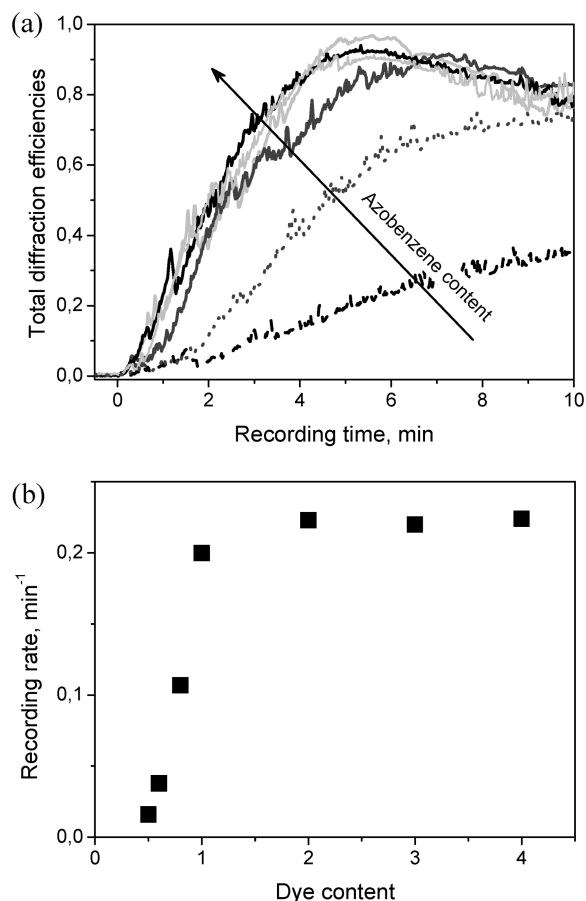
FIGURE 8. Efficiency of gratings formation in dependence on the azobenzene content: (a) kinetics of total diffraction efficiencies; (b) recording rates. The MR:APTES ratio was varied as indicated (catalytic amount of HCl).

limited dye loading, typically to 10 %. Only for specially synthesized dyes with higher solubility in polymer matrix has dye loading as high as 30 % been reported. The dye loading of 100 % could be reached only by covalent bonding the chromophores to the polymer matrix, whereas the dye aggregation has been effectively suppressed. But even in covalently bound systems, the aggregation of chromophores is not completely excluded and can hinder the SRG formation as it was shown on a series of functionalized polymers (25). Intermolecular interactions, such as ionic and H-bonding, present another way to reduce the tendency of the molecules to aggregate (26). The presence of strong noncovalent interactions allowed the loading level, which typically has been achieved only by covalent bonding of the dye molecules to the polymer. In this study, we have varied MR content in the mixture from 0.5 to 4 azobenzene chromophores for each APTES unit. SRG were inscribed onto films of each material under identical experimental conditions described above. The formation of SRG was characterized by the total diffraction efficiencies measured during the grating recording. The kinetics are shown in Figure 8a. With increasing azobenzene content, the grating formation becomes faster, i.e., more effective, until MR:APTES ratio of 1:1 is reached. Further increasing of chromophores content did not lead to any improvement of the grating recording. This is clearly seen in Figure 8b, where the gratings rates
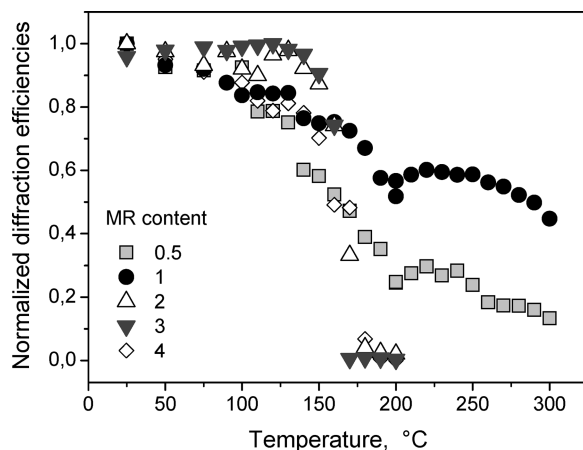
FIGURE 9. Thermal stability of SRG in materials with different dye content: temperature dependence of the normalized total diffraction efficiencies. MR:APTES ratio was varied as 0.5:1, 1:1, 2:1, 3:1, and 4:1 (catalytic amount of HCl).

estimated from the kinetics for different materials of the series are mapped in dependence on the MR:APTES ratio. Notice, that the comparison of the relief gratings by their diffraction efficiencies is burdened with some errors. The errors are caused by the induced phase volume grating and by the difference of refractive indices of materials with different azobenzene content. However, for the materials under study, these errors do not exceed 5 %. An explanation of the dependence on azobenzene content requires more detailed investigations, including consideration of complexation and aggregation. Here, we just give some thoughts to this effect. The increase in grating formation efficiency with increasing azobenzene content is well-expected because the photoisomerization of azobenzene is considered to be the driving force of the SRG formation. The saturation behavior at the MR:APTES ratio exceeding 1:1 ratio could have a few reasons. If bound to the passive polymer chains, the chromophores involve the latter into their motion. If the amount of azobenzene exceeds the amount of bonding sites (protonated amino group of APTES) the chromophores remain unbound. These "free" chromophores still can be moved by light, but their movement is not necessarily accompanied by the transfer of polymer matrix. Beyond, the presence of "free" units has a plasticizing effect enhancing the relaxation of any induced order. Also the aggregation of azobenzene becomes quite probable at higher MR:APTES ratios. All these factors destructively affect the SRG formation and can explain the observed dependence on MR:APTES ratio.

3.5. Effect of MR:APTES Ratio on Thermal Stability of SRG.
The above assumption that the presence of the exceeding azobenzene units essentially changes the film properties can be proved by investigation of the thermal stability of the inscribed relief structures in dependence on the MR:APTES ratio. In this study, the gratings inscribed in films with MR:APTES ratios varying from 0.5:1 to 4:1 were erased by heating the samples. We used here the same heating procedure as described above for differently treated films. The normalized total diffraction efficiencies in dependence on the annealing temperatures are presented in Figure 9. It can be seen that the erasure behavior essentially
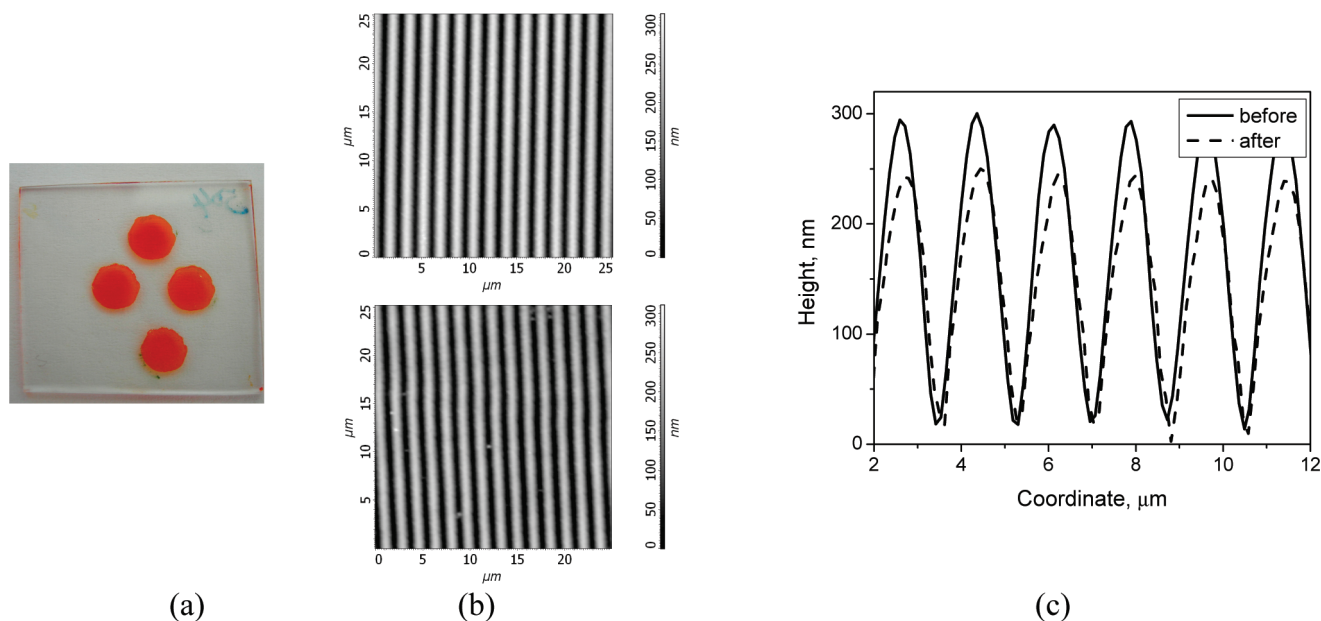
FIGURE 10. (a) Photograph of the film rinsed in water: bottom spot was irradiated homogeneously, three upper spots, with interference pattern; (b) AFM images of one of the gratings before (top) and after (bottom) rinsing the film; (c) corresponding cross-sections of the grating.

changes if the MR:APTES ratio exceeds 1:1 ratio. The gratings in the materials with higher azobenzene contents remain stable up to the temperature of about 140 °C and then drop within a temperature interval of 30°. Heating to a temperature of 180 °C erases the gratings completely. On the contrary, gratings in the materials with lower azobenzene content erase gradually with diffraction efficiencies remaining at the level of 30−60% of their initial values after being heated up to the temperatures of 190 °C, at which point the peculiarity in the erasure curve is seen. Notice that this temperature correlates with an exothermic peak in the DSC curve (Figure 7). The gratings could not be erased anymore by further heating the samples up to 300 °C. For example, 45% of the initial diffraction efficiency of the grating remained in the case of the material with a 1:1 MR: APTES ratio.

The cross-linking inherent to the sol−gel materials and its effect on the formation and stability of SRG in the supramolecular ionic azobenzene sol−gel materials has been discussed above. If the light-induced mass transport is known to be optically and thermally reversible, the silane component undergoing the condensation reaction grants the irreversibility to the material. The catalyst concentration can change the velocity of the cross-linking process and thus define the degree of cross-linking.

3.6. Light-Induced Insolubility. Here we have observed another interesting phenomenon. The properties of material composed of MR and APTES could be manipulated by the irradiation with light. If a film was irradiated with actinic light, the solubility of the film was changed, namely the irradiated film became insoluble in water or ethanol. In the experiment, four spots were irradiated onto the film either homogeneously or with an interference pattern as described above for the recording of SRG. After the irradiation of all spots was complete, the film was rinsed with water or alternatively with ethanol. A picture of the rinsed film is shown in Figure 10a. It is clearly seen that the film was completely washed out the glass substrate with the exception of the irradiated areas. Thus the initially well-soluble film becomes insoluble because of irradiation. As concerns the inscribed relief gratings, rinsing the film caused a small lowering of the relief height from initially 280 to 230 nm. Figure 10b shows the AFM images of one of the inscribed gratings before and after rinsing the film and Figure 10c presents corresponding cross-sections of the grating. To the best of our knowledge, such reaction has not been described in the literature; thus the explanation of the effect requires detailed theoretical and experimental studies. What comes first in mind is an advancement of sol−gel condensation reaction of the APTES accelerated by some acid/base catalyst during exposure by the azobenzene component undergoing *E/Z* isomerization. The acidity/basicity of organic compounds can be changed in excited state by few order of magnitude (27). Possibly, this makes one of the components of formulation (e.g., amine, carboxylic acid, carboxylate anion) stronger catalyst. Another possible reaction also leading to insolubility in water and alcohol is the photochemical formation of amide (covalent bonding between MR and APTES), shown by the appearance of carbonyl vibration at 1670 cm^{-1} in FTIR spectrum.

4. CONCLUSIONS

In summary, we have shown that very deep SRG, with relief height up to 750 nm at a period of 2 μm, can be recorded in sol−gel-based material in a relatively short time. The difference from other azobenzene-containing materials is that light-induced mass transport in this material is strongly influenced by the cross-linking of siloxane chains. This fact forced us to reconsider the grating formation process involving for the first time some new macro parameters and processes such as residual solvent content, plasticizing or relaxation effects. We have applied different

drying procedures to the films and have shown that the residual solvent content can affect both induction and stability of the molecular orientation. We have also shown that the thermal stability of the light-induced structures in this material can be significantly improved by proper thermal treatment— aging and drying—of the films.

We have clearly demonstrated that increasing chromophore content favorably affects the mass transport until their amount exceeds the amount of counterion matrix units. Plasticizing effect of azobenzene, decoupling of exceeding chromophores from the matrix or their aggregation have been suggested as possible reasons for the saturation effect. The investigation of the thermal erasure of gratings has shown that it depends strongly on film treatment and the MR:APTES ratio. Comparison of the erasure processes revealed two characteristic temperatures that correlate with the DSC curves of the material.

For the first time, we have shown that the solubility of films may be affected by the photoreaction of azobenzene chromophore in this matrix. That means that initially soluble films turn insoluble if irradiated with light.

REFERENCES AND NOTES

(1) Rochon, P.; Batalla, E.; Natansohn, A. *Appl. Phys. Lett.* **1995**, *66*, 136. Kim, D. Y.; Tripathy, S. K.; Li, L.; Kumar, J. *Appl. Phys. Lett.* **1995**, *66*, 1166.

(2) Zhao, Y.; Ikeda, T., Eds. *Smart Light-Responsive Materials. Azobenzene-Containing Polymers and Liquid Crystals*; John Wiley & Sons: New York, 2009.

(3) Natansohn, A.; Rochon, P. *Chem. Rev.* **2002**, *102*, 4139.

(4) Lagugné-Labarthet, F.; Buffeteau, T.; Sourisseau, C. *J. Phys. Chem. B* **1998**, *102*, 2654. Fukuda, T.; Kim, J. Y.; Barada, D.; Yase, K. *Proc. SPIE* **2006**, *6136*, 61360Y. Ke, X.; Yan, X.; Song, S.; Li, D.; Yang, J. J.; Wang, M. R. *Opt. Mater.* **2007**, *29*, 1375.

(5) Oliveira, J.; Osvaldo, N.; dos Santos, J.; David, S.; Balogh, D. T.; Zucolotto, V.; Mendonca, C. R. *Adv. Colloid Interface Sci.* **2005**, *116*, 179.

(6) Zakrevskyy, Y.; Stumpe, J.; Smarsly, B.; Faul, C. F. J. *Phys. Rev. E* **2007**, *75*, 031703. (a) Zakrevskyy, Y.; Stumpe, J.; Faul, C. F. J. *Adv. Mater.* **2006**, *18*, 2133.

(7) Viswanathan, N. K.; Kim, D. Y.; Bian, S.; Williams, J.; Liu, W.; Li, L.; Samuelson, L.; Kumar, J.; Tripathy, S. K. *J. Mater. Chem.* **1999**, *9*, 1941.

(8) Boilot, J. P.; Biteau, J.; Chaput, F.; Gacoin, T.; Brun, A.; Darracq, B.; Georges, P.; Levy, Y. *Pure Appl. Opt.* **1998**, *7*, 169.

(9) Darracq, B.; Chaput, F.; Lahlil, K.; Lévy, Y.; Boilot, J.-P. *Adv. Mater.* **1998**, *10*, 1133.

(10) Fiorini, C.; Prudhomme, N.; de Veyrac, G.; Maurin, I.; Raimond, P.; Nunzi, J.-M. *Synth. Met.* **2000**, *115*, 121.

(11) Ishow, E.; Lebon, B.; He, Y.; Wang, X.; Bouteiller, L.; Galmiche, L.; Nakatani, K. *Chem. Mater.* **2006**, *18*, 1261.

(12) Barrett, C.; Natansohn, A.; Rochon, P. *J. Phys. Chem.* **1996**, *100*, 8836.

(13) Kulikovska, O.; Goldenberg, L. M.; Stumpe, J. *Chem. Mater.* **2007**, *19*, 3343.

(14) Stumpe, J.; Goldenberg, L.; Kulikovska, O. European patent EP 1 794 236 B1, 2008.

(15) Kulikovska, O.; Goldenberg, L. M.; Kulikovsky, L.; Stumpe, J. *Chem. Mater.* **2008**, *20*, 3528.

(16) Gao, J.; He, Y.; Xu, H.; Song, B.; Zhang, X.; Wang, Z.; Wang, X. *Chem. Mater.* **2007**, *19*, 14. Gao, J.; He, Y.; Liu, F.; Zhang, X.; Wang, Z.; Wang, X. *Chem. Mater.* **2007**, *19*, 3877. Zettsu, N.; Ogasawara, T.; Mizoshita, N.; Nagano, S.; Seki, T. *Adv. Mater.* **2008**, *20*, 516.

(17) Zhang, Q.; Bazuin, C. G.; Barrett, C. J. *Chem. Mater.* **2008**, *20*, 29.

(18) Chaput, F.; Lahlil, K.; Biteau, J.; Boilot, J.-P.; Darracq, B.; Levy, Y.; Peretti, J.; Safarov, V. I.; Lehn, J.-M.; Fernandez-Acebes, A. *Proc. SPIE* **2000**, *3943*, 32.

(19) Frey, L.; Darracq, B.; Chaput, F.; Lahlil, K.; Jonathan, J. M.; Roosen, G.; Boilot, J. P.; Levy, Y. *Opt. Commun.* **2000**, *173*, 11. Kim, M.-R.; Choi, Y.-I.; Park, S.-W.; Lee, J.-W.; Lee, J.-K. *J. Appl. Polym. Sci.* **2006**, *100*, 4811.

(20) Rosenhauer, R.; Kulikovsky, L. 2009, personal communication.

(21) Jeong, S.; Kim, D.; Park, B. K.; Lee, S.; Moon, J. *Nanotechnology* **2007**, 025204.

(22) Zucolotto, V.; Barbosa Neto, N. M.; Rodrigues, J. J., Jr.; Constantino, C. J. L.; Zílio, S. C.; Mendonça, C. R.; Aroca, R. F.; Oliveira, O. N., Jr. *J. Nanosci. Nanotechnol.* **2004**, *4*, 855. Zucolotto, V.; He, J.-A.; Constantino, C. J. L.; Barbosa Neto, N. M.; Rodrigues, J.; Jose, J.; Mendonca, C. R.; Zilio, S. C.; Li, L.; Aroca, R. F.; Oliveira, O. N.; Kumar, J. *Polymer* **2003**, *44*, 6129.

(23) Cojocariu, C.; Rochon, P. *Pure Appl. Chem.* **2004**, *76*, 1479. Yager, K. G.; Barrett, C. *Macromolecules* **2006**, *39*, 9320.

(24) Goldenberg, L. M.; Kulikovska, O.; Stumpe, J. *Langmuir* **2005**, *21*, 4794.

(25) Börger, V.; Kulikovska, O.; G.-Hubmann, K.; Stumpe, J.; Huber, M.; Menzel, H. *Macromol. Chem. Phys.* **2005**, *206*, 1488.

(26) Priimagi, A.; Cattaneo, S.; Ras, R. H. A.; Valkama, S.; Ikkala, O.; Kauranen, M. *Proc. SPIE* **2006**, *6192*, 61922U1. Priimagi, A.; Cattaneo, S.; Ras, R. H. A.; Valkama, S.; Ikkala, O.; Kauranen, M. *Chem. Mater.* **2005**, *17*, 5798. Priimagi, A.; Kaivola, M.; Rodriguez, F. J.; Kauranen, M. *Appl. Phys. Lett.* **2007**, *90*, 121103. Priimagi, A.; Vapaavuori, J.; Rodriguez, F. J.; Faul, C. F. J.; Heino, M. T.; Ikkala, O.; Kauranen, M.; Kaivola, M. *Chem. Mater.* **2008**, *20*, 6358.

(27) Wayne, R. P. *Principles and Applications of Photochemistry*, 2nd ed.; Oxford University Press: New York, 1988.

AM900283A